Nuclear Engineering and Technology 52 (2020) 2119–2129

Contents lists available at ScienceDirect

Nuclear Engineering and Technology

journal homepage: www.elsevier.com/locate/net

Original Article

Development of wall-thinning evaluation procedure for nuclear power plant piping - Part 2: Local wall-thinning estimation method

Hun Yun [a], Seung-Jae Moon [b, **], Young-Jin Oh [a, *]

[a] KEPCO Engineering and Construction Co., Ltd. 269 Hyeoksin-ro, Gimcheon-si, Gyeongsangbuk-do, 39660, Republic of Korea
[b] Department of Mechanical Engineering, Hanyang University, 222 Wangsimni-ro, Seongdong-gu, Seoul, 04763, Republic of Korea

ARTICLE INFO

Article history:
Received 7 January 2020
Received in revised form
21 February 2020
Accepted 2 March 2020
Available online 13 March 2020

Keywords:
Wall-thinning
Thickness inspection
Wall-thinning estimation
Statistical significance

ABSTRACT

Flow-accelerated corrosion (FAC), liquid droplet impingement erosion (LDIE), cavitation and flashing can cause continuous wall-thinning in nuclear secondary pipes. In order to prevent pipe rupture events resulting from the wall-thinning, most NPPs (nuclear power plants) implement their management programs, which include periodic thickness inspection using UT (ultrasonic test). Meanwhile, it is well known in field experiences that the thickness measurement errors (or deviations) are often comparable with the amount of thickness reduction. Because of these errors, it is difficult to estimate wall-thinning exactly whether the significant thinning has occurred in the inspected components or not. In the previous study, the authors presented an approximate estimation procedure as the first step for thickness measurement deviations at each inspected component and the statistical & quantitative characteristics of the measurement deviations using plant experience data. In this study, statistical significance was quantified for the current methods used for wall-thinning determination. Also, the authors proposed new estimation procedures for determining local wall-thinning to overcome the weakness of the current methods, in which the proposed procedure is based on analysis of variance (ANOVA) method using sub-grouping of measured thinning values at all measurement grids. The new procedures were also quantified for their statistical significance. As the results, it is confirmed that the new methods have better estimation confidence than the methods having used until now.

1. Introduction

Flow-accelerated corrosion (FAC), liquid droplet impingement erosion (LDIE), cavitation and flashing are active degradation mechanisms that damage the pipes of nuclear secondary systems. These kinds of degradation occur as wall-thinning phenomenon at local areas of piping components, such as pipes, elbows, tees, reducers, etc. The wall-thinning can cause eventually leaks or ruptures in pressure boundary of nuclear power plants (NPPs). Several fatal failures have been reported at some nuclear power plants in the world since the accident at Surry NPP in 1981. In order to prevent pipe rupture events, many research programs, especially for FAC, have been conducted over 40 years, then many research reports were published and pipe wall thinning management procedures were made [1–3].

As introduced in the previous study [4], the management activity to prevent pipe rupture events due to wall-thinning, includes 'initial predictions of thinning rates', 'periodic inspections' and 'residual life predictions based on the inspections'. Therefore, the reliable analysis and decisions for the inspection are very important to prevent pipe rupture. Nevertheless, the inspections results, which are conducted by ultrasonic thickness measurements (see Fig. 1), contain significant levels of measurement uncertainty as shown in the previous study [4]. This measurement error makes over-conservative prediction for wall-thinning rates and, sometimes, makes it difficult to estimate whether the significant thinning occurs or not in the inspected components.

Currently, several thinning estimation methods are used in pipe wall-thinning management programs, which were developed by EPRI (Electric Power Research Institute) and CHUG (CHECWORKS User Group) members [5–14]. However, the reliabilities or statistical significances of the estimation methods have not been presented systematically. In a previous research for the thinning estimation method [15], the reliability of the method was

* Corresponding author. Tel.: 82 54 421 6463; fax: 82 54 421 6462.
** Corresponding author.
E-mail addresses: smoon@hanyang.ac.kr (S.-J. Moon), yjoh2@kepco-enc.com (Y.-J. Oh).

https://doi.org/10.1016/j.net.2020.03.001

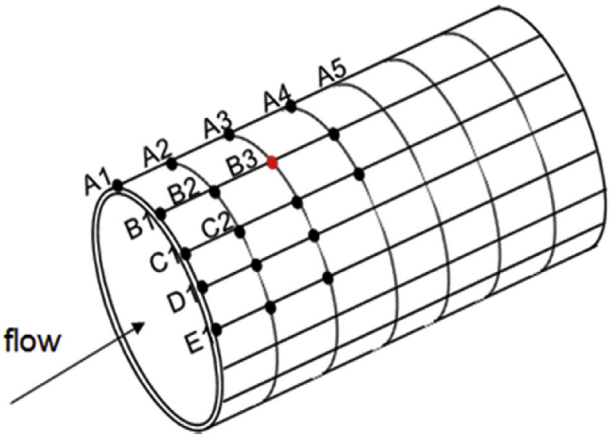

(a) Example of surface grids for UT inspection

(b) UT inspection during a plant outage

Fig. 1. Thickness measurement using UT (ultrasonic test) for pipe wall thinning management.

examined, in which the considerable level of estimation success probability is shown only in very deeply thinned cases. In this paper, the statistical significance of currently used methods was examined, and then some more reliable estimation procedures are proposed for the pipe wall-thinning estimation using thickness measurement results.

2. Review of current methodologies for wall-thinning estimation

2.1. Total point method (TPM)

Total point method (TPM) is one of the thinning determination methods proposed by EPRI [11,12]. TPM uses the measured values of thickness reduction (thinning) in all grid positions of a component. The thinning values can be determined by thickness differences in periodically measured thickness values for 2-time inspections or least square fitting slopes for 3-time or more inspections. A histogram can be constructed by using all of the thinning values. The thinning estimation can be made by the shape of the histogram. If the mode in the histogram is clearly greater than zero (see Fig. 2 (a)), TPM judges that thinning occurs. Conversely, if the mode is near zero or clearly smaller than zero (see Fig. 2 (b)), it is judged that thinning does not occur.

From many field experiences, it is well known that FAC or other kinds of thinning mechanism occur not in the whole area but in a local area. If local thinning occurs, the histogram will show two peak values, i.e., nearly at zero and a certain positive value (see Fig. 2 (c)). Although the shape of the histogram, whether there are two peaks or not, is the most important in TPM, the judgement is somewhat ambiguous because the shape of the histogram is significantly dependent on the bin size. In order to resolve this ambiguity, the authors proposed a numerical method for the histogram estimation in the previous study [15].

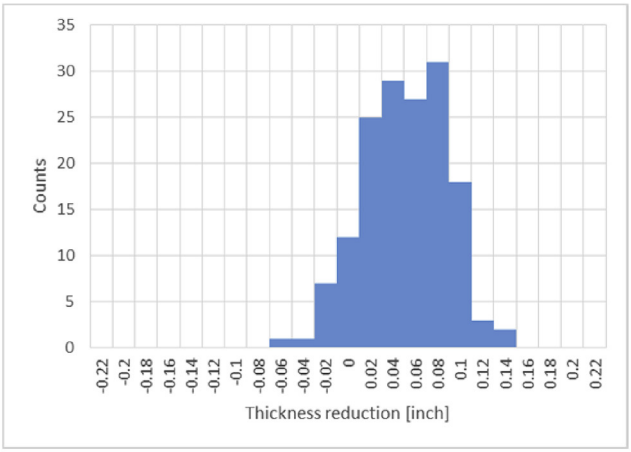

(a) Uniform thinning

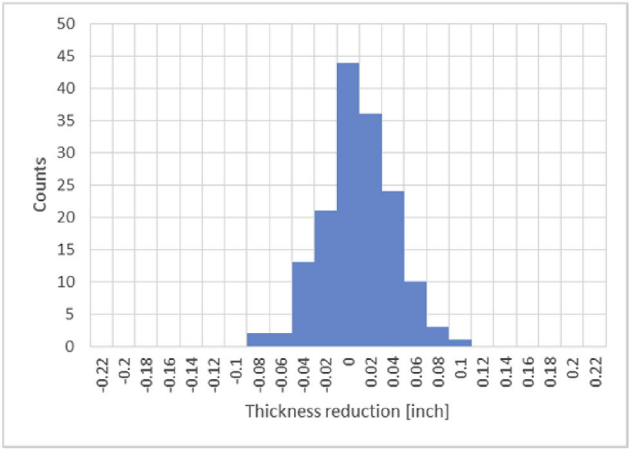

(b) Not thinning

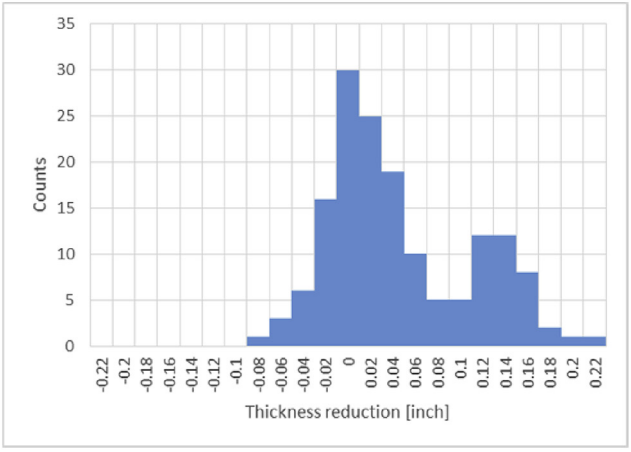

(c) Local thinning

Fig. 2. Thinning evaluation by TPM using histograms of measured thickness reduction values.

	Treatment-1	Treatment-2	...	Treatment-k
Specimen-1	y_{11}	y_{21}	...	y_{k1}
Specimen-2	y_{12}	y_{22}	...	y_{k2}
Specimen-3	y_{13}	y_{23}	...	y_{k3}
...	...	...	...	...
Specimen-n	y_{1n}	y_{2n}	...	y_{kn}
Partial mean	$\bar{y}_{1\cdot}$	$\bar{y}_{2\cdot}$	...	$\bar{y}_{k\cdot}$
Total mean	$\bar{y}_{\cdot\cdot}$			

< Hypothesis >

H_0 : No effect of treatments on specimens. For all i, $y_{i\cdot}=\bar{y}_{\cdot\cdot}$

H_1 : Significant effects of treatments on specimens. For certain i, $y_{i\cdot}\neq\bar{y}_{\cdot\cdot}$

Fig. 3. Schematics of one-way ANOVA for treated specimen experiments.

Although the proposed method can reduce some degrees of ambiguity, TPM still has a significant weakness such that it does not consider the location where local thinning occurs. If a certain positive peak between 2 peaks of the histogram is proved to be local thinning, the peak value and the similar high values should be located locally together. TPM does not use the location information of the thinning values.

2.2. Analysis of variance (ANOVA)

Analysis of variance (ANOVA) is a commonly used statistical model to analyze the differences among group means [16,17]. For instance, an experimental example can be considered. In order to estimate the differences among treatments, n-number of specimens was tested, in which k-number of treatments was considered, as shown in Fig. 3. The differences of test results among treatments can be detected. However, there will probably be differences and deviations within the test results of one treatment, too. Therefore, we have to use any criterion to estimate whether there are

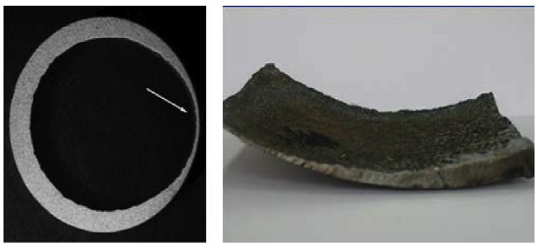

Fig. 5. An example for pipe wall thinning occurred at a local area.

significant differences among treatments or not. In this case, the one-way ANOVA method can be applied to the estimation, wherein the following statistical estimator is used to test the hypothesis summarized in Fig. 3.

$$f = \frac{MS_{tr}}{MSE}, \qquad \text{(Eq. 1)}$$

$$MS_{tr} = \frac{n\sum_{i=1}^{k}(\bar{a}_{i\bullet} - \bar{a}_{\bullet\bullet})^2}{k-1},$$

$$MSE = \frac{\sum_{i=1}^{k}\sum_{j=1}^{n}(a_{ij} - \bar{a}_{i\bullet})^2}{n-k},$$

where, f is the test statistic for the one-way ANOVA, MS_{tr} is treatment mean of squares, MSE is mean square error, a_{ij} is a test result of the j-th specimen and the i-th treatment, n is the number of specimens, k is the number of treatments, $\bar{a}_{i\bullet}$ is the partial mean of a_{ij} for each treatment, and $\bar{a}_{\bullet\bullet}$ is the total mean of a_{ij}.

The following criteria can be used to make decisions for the hypothesis testing.

- There is no difference of treatment means on specimens, if $f < F_{\alpha}(k-1, kn-k)$,
- There are significant differences among treatments, if $f \geq F_{\alpha}(k-1, kn-k)$,

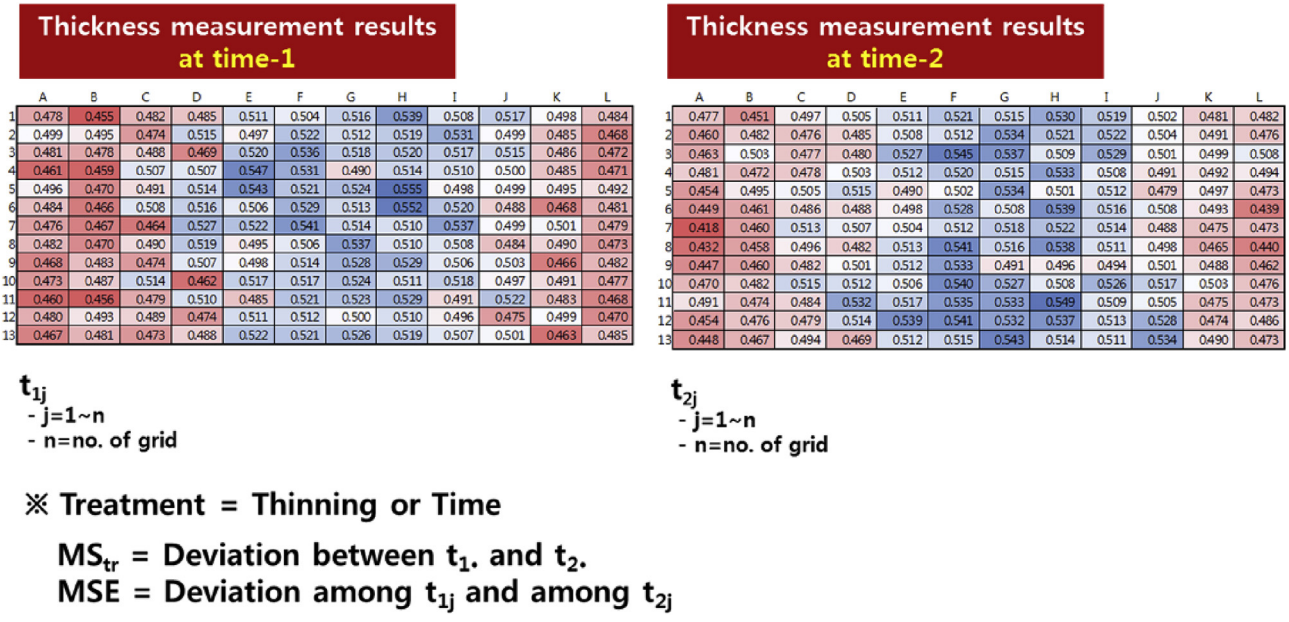

Fig. 4. EPRI's approach to estimate pipe wall thinning using ANOVA.

	A	B	C	D	E	F	G	H	I	J	K	L
1	0	0	0	0	0	0	0	0	0	1	0	0
2	1	0	0	0	0	0	0	0	1	0	0	0
3	0	0	0	0	0	0	0	0	0	0	0	0
4	0	0	0	0	0	0	0	0	0	0	0	0
5	0	0	0	0	0	0	0	0	0	0	0	0
6	0	0	0	0	0	0	0	0	0	0	0	1
7	0	0	0	0	0	0	0	0	0	0	0	0
8	1	0	0	1	0	0	0	0	0	0	0	0
9	0	0	0	0	0	0	0	1	0	0	0	0
10	0	0	0	0	0	0	0	0	1	0	0	0
11	0	0	0	0	0	0	0	0	0	0	0	0
12	0	1	0	0	0	0	0	0	0	0	0	0
13	0	0	0	1	0	0	0	0	0	0	0	0

(a) Uniform thinning example

	A	B	C	D	E	F	G	H	I	J	K	L
1	0	0	0	0	0	0	0	0	0	0	0	0
2	1	0	0	0	0	0	0	0	0	0	0	0
3	0	0	0	0	0	0	0	0	0	0	0	0
4	0	0	0	0	0	0	0	0	0	0	0	1
5	0	0	0	0	0	0	0	0	0	0	0	0
6	1	1	0	0	0	0	0	0	0	0	0	1
7	0	0	0	0	0	0	0	0	0	0	0	0
8	1	0	1	0	0	0	0	0	0	0	1	0
9	1	0	0	0	0	0	0	0	0	0	0	0
10	0	0	0	0	0	0	0	0	0	0	0	1
11	0	0	0	0	0	0	0	0	0	0	0	0
12	0	0	0	0	0	0	0	0	0	0	0	0
13	0	0	0	0	0	0	0	0	0	0	0	0

(b) Local thinning example

Fig. 6. Examples of grid location distribution for 10 upper values of thinning depth.

Where, $F_{\alpha}(k-1, kn-k)$ is F-distribution whose degrees of freedom are $k-1$ and k$n-k$, and α is the level of significance.

In EPRI report [11], the one-way ANOVA is proposed as the thinning estimation method by substituting 'time' for 'treatment'. As summarized in Fig. 4, the thickness measurement data in n-number of grids at time-1 are defined as the data of treatment-1. The data at time-2 are defined as the data of treatment-2. In other words, a_{ij} is t_{ij}, which is the measured thickness at the i-th time and the j-th grid in the EPRI's ANOVA method. If f value is larger than $F_{\alpha}(k-1, kn-k)$, it means that thickness reduction occurs between time-1 and time-2 data.

The EPRI's approach using ANOVA can be simple and effective to estimate thinning. However, it overlooks the characteristics of systematic thickness distributions of pipe fittings such as elbows or tees. In general, the thickness of a manufactured pipe fitting is not uniform. In the case of an elbow manufactured by bending processes, the thickness at the intrados area is 1.2 or more times thicker than the thickness at the extrados area. In this case, there are large thickness deviations among the measured values at each time even if there are ignorable measurement errors. These deviations make the *MSE* value larger, which reduce f values in Eq. (1). This can make incorrect estimations that thinning does not occur even though significant thinning occurs. Also, this approach may not work well in local thinning because it considers the thickness changes over the entire area.

3. Development of local wall-thinning estimation method

Considering field experiences dealing with pipe wall-thinning of nuclear secondary systems [1], in most cases, significant thinning has occurred at a local area of piping components (see Fig. 5). The uniform thinning on the inner surface can be easily estimated by comparing the average of thickness values at each time or TPM as shown in Fig. 2 (a). In case of local thinning, however, the estimation accuracy of TPM decreases as shown in the previous study [15]. Also, the EPRI's approach using ANOVA does not work well in the local thinning as explained at Section 2 of this paper.

Considering these situations, new methodologies were proposed in this paper for estimating local wall-thinning, and their estimation performance was examined. In order to estimate the local thinning, this study focused on finding effective ways to use the location information of the measurement data. The proposed methods can be used to estimate whether the local wall-thinning was occurred or not.

3.1. Locational deviation method (LDM)

As the first attempt to use the location information, a parameter for location deviations of the significantly thinned grids was considered. If the thinning occurs uniformly, the locations where thinning occurs will be evenly distributed. If the measured values contain random errors, high values will be randomly distributed,

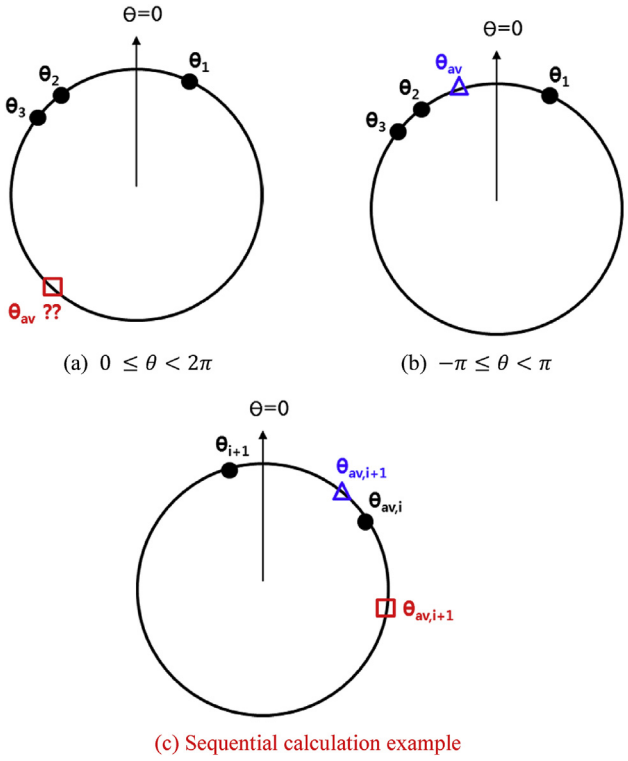

Fig. 7. Dependency of average values of circumferential locations on angular range definitions.

and the location deviation of these data will be large. If the thinning occurs in a local area, the high values will exist locally. Then, the location deviation of locally thinned grids will be small. In order to determine whether local thinning occurs or not, upper values of measured thinning were used in this study. Fig. 6 shows an example of 10 upper thinning values.

If the geometrical shape of the grids is rectangular rather than cylindrical, the Cartesian coordinates can be used to define locational deviation as follows:

$$\mathrm{Std}(x)^2 = \frac{\sum_{i=1}^{n}(x_i - x_{av})^2}{n-1}, \mathrm{Std}(y)^2 = \frac{\sum_{i=1}^{n}(y_i - y_{av})^2}{n-1}, \quad \text{(Eq. 2)}$$

$$x_{av} = \frac{\sum_{i=1}^{n} x_i}{n}, y_{av} = \frac{\sum_{i=1}^{n} y_i}{n}, \quad \text{(Eq. 3)}$$

where, x_i and y_i are the i-th grid locations for Cartesian coordinates. Std(x) and Std(y) are standard deviations of x and y, respectively. x_{av} and y_{av} are average values for x_i and y_i. n is the total number of grids for upper bound thinning values.

In the case of pipe fittings, however, circumferential direction is a circle not a straight line. For this reason, a specific treatment to define the average of circumferential location is needed. For example as shown in Fig. 7 (a), there are three values of angle (θ_1, θ_2, θ_3). When we use a simple method with definition for angle range, ($0 \le \theta_1 < 2\pi$), the average for θ_i is placed at the red rectangle mark in Fig. 7 (a). Considering the intension of average, which minimizes the standard deviation, the average for θ_i is placed at the blue triangle mark in Fig. 7 (b). In order to avoid the cases like Fig. 7(a), the authors made a modified sequential procedure to calculate average value of θ_i.

In general, average value calculation equation (Eqs. (4)–(1)), is equivalent with a sequential equation, (Eqs. (4)–(2)).

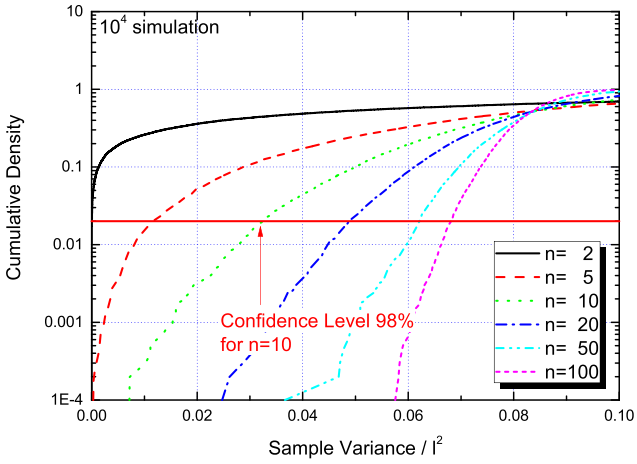

Fig. 8. Monte-Carlo simulation results for location variances of uniformly distributed points in a line (l = length of the line, n = number of sample points).

$$\theta_{av} = \frac{\sum_{i=1}^{n}\theta_i}{n} \quad (4-1)$$

Where, θ_i is the i-th circumferential location of a thinned grid, and θ_{av} is the average of θ_i.

$$\text{For} \cdot i = 1 \sim n-1 \cdot \theta_{av,i+1} = \frac{i\theta_{av,i} + \theta_{i+1}}{i+1}\theta_{av} = \theta_{av,n}, \quad (4-2)$$

Where, $\theta_{av,i}$ means the partial average for the data of $\theta_{av,1} \sim \theta_{av,i}$.

When the range of angle is defined by ($0 \le \theta < 2\pi$) and the i-th partial average, $\theta_{av,i}$ and the (i+1)-th angle, θ_{i+1} are located shown at Fig. 7(c), the (i+1)-th partial average, $\theta_{av,i+1}$ calculated using (Eqs. (4)–(2)) is located at the red rectangle mark of Fig. 7(c). In the engineering view point, the (i+1)-th partial average, $\theta_{av,i+1}$ has to be located at the blue triangle mark, considering that average values minimize the standard deviations. In order to resolve these inadequacies, θ_{i+1} is transformed to the difference from $\theta_{av,i}$ shown in (Eqs. (4)–(3)), then the angle range is calibrated to the range of ($-\pi \le \theta < \pi$) shown in (Eq. (5)).

$$\theta_{av,i+1} = \frac{i\theta_{av,i} + \theta_{i+1}}{i+1}, = \theta_{av,i} + \frac{\Delta\theta_{i+1}}{i+1}, \Delta\theta_{i+1} = \theta_{i+1} - \theta_{av,i}, \quad \text{(Eq. 4-3)}$$

$$\theta' = \begin{cases} \theta + 2\pi & for \ -2\pi < \theta \le -\pi \\ \theta & for \ -\pi < \theta \le \pi \\ \theta - 2\pi & for \ \pi < \theta \le 2\pi \end{cases} \quad \text{(Eq. 5)}$$

Where, θ is the value of $\theta_{av,i}$ or $\Delta\theta_{i+1}$ before calibration, and θ' is the calibrated value for θ. From the cumulative calculation using Eqs. (4) and (5), the average value for the circumferential location of thinned grids, θ_{av} can be determined as follows:

$$\theta_{av} = \theta_{av,n} \quad \text{(Eq. 6)}$$

Using Eq. (2) and Eq. (6), the locational standard deviations of thinned grids, Std(θ) and Std(z) can be determined, where θ and z are circumferential and axial coordinates for grids. Then, if the deviation is smaller than a decision criterion, it can be concluded that local thinning occurs. The decision criterion can be determined to be a lower bound value of the locational standard deviations for uniformly distributed locations.

In this study, simple Monte-Carlo (MC) simulations were

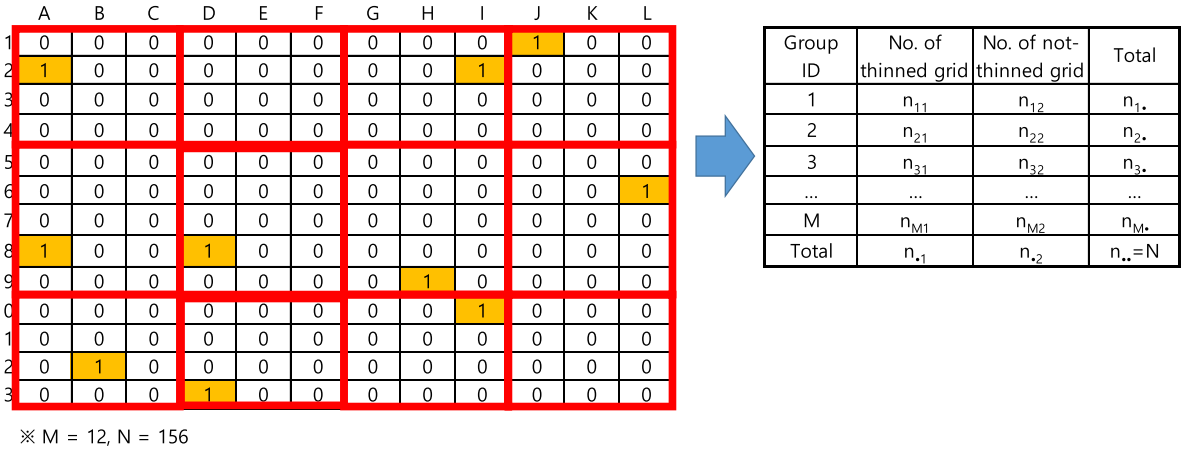

Group ID	No. of thinned grid	No. of not-thinned grid	Total
1	n_{11}	n_{12}	$n_{1\bullet}$
2	n_{21}	n_{22}	$n_{2\bullet}$
3	n_{31}	n_{32}	$n_{3\bullet}$
...	...	...	...
M	n_{M1}	n_{M2}	$n_{M\bullet}$
Total	$n_{\bullet 1}$	$n_{\bullet 2}$	$n_{\bullet\bullet}=N$

Fig. 9. Schematics of binomial variables uniformity test (BVUT) using locational grid groups.

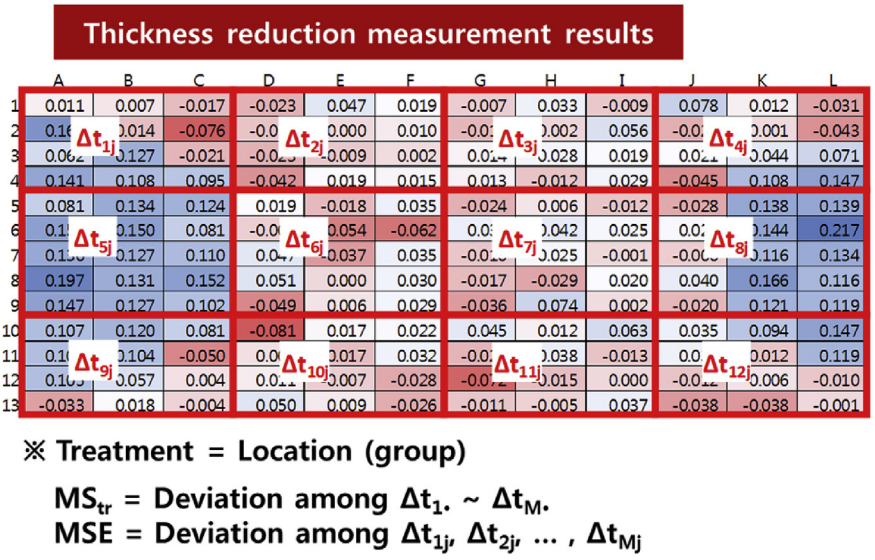

Fig. 10. Schematics of continuous variables uniformity test (CVUT) using locational grid groups and one-way ANOVA.

conducted for various numbers of samples. Fig. 8 shows the cumulative density of the sample variance (= square of standard deviation) for uniformly distributed locations calculated from the MC simulations for various numbers of samples, n, where the sample variances were normalized by a length of line for the location. As shown in Fig. 8, a 98% lower bound for sample variance increases as the number of samples increases. For n = 10, the 98% lower bound value is 0.32, and this value was used as the decision criterion in this study.

3.2. Binomial variables uniformity test (BVUT) method

In the second try to estimate local thinning, a locational grouping methodology was used. As shown in Fig. 9, the measurement grids can be divided into several groups. If thinning occurs uniformly, there will be similar numbers of thinned grids in all groups. In this method, the thinning value at each grid needs to be converted into a binomial value, generally "1" or "0", meaning to be thinned or not-thinned.

Various kinds of criteria can be used in this conversion. In the study, the 10% upper bound value of thinning values of a component were used as a dividing criterion. If a thinning value of a grid is greater than the 10% upper bound of thinning values of the component, the thinning value is converted to "1", which mean probably thinned in the grid location. If not, then the thinning values is converted to "0", which mean probably not thinned in the grid location. This conversion has an intension of thinning distribution estimation, but does not have meaning it is confident there is significant thinning in a grid.

After N grids are divided into M groups as shown in Fig. 9, count the number of selected grids. Each group can be categorized by thinned and not-thinned numbers. In this case, the χ^2 hypothesis test can be used to estimate whether the number of thinned grids is similar in all groups or not. Assuming that N grids are divided into M groups, the number of thinned grids can be defined as n_{m1}, while the number of not-thinned grids is n_{m2}. Test statistics, T, can be calculated by Eq. (7) as follows:

$$T = \sum_{m=1}^{M} \sum_{j=1}^{2} \frac{\left(n_{mj} - \left(n_{m\bullet} n_{\bullet j}\right)/N\right)^2}{\left(n_{m\bullet} n_{\bullet j}\right)/N}, \qquad \text{(Eq. 7)}$$

where, $n_{m\bullet}$ and $n_{\bullet j}$ mean $\sum_j n_{mj}$ and $\sum_m n_{mj}$, respectively. According

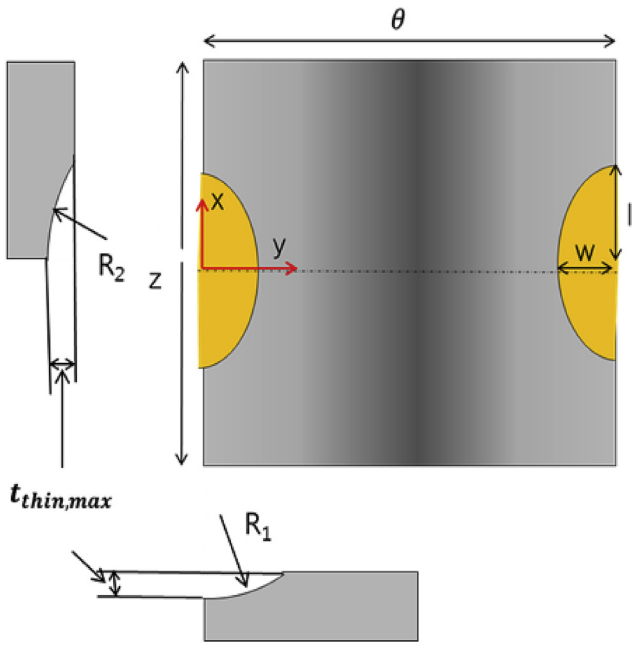

Fig. 11. Local thinning shape of virtual thinned pipes for Monte-Carlo probability tests.

to the general procedure for χ^2 test, presence of local wall-thinning can be estimated as follows:

- Local wall-thinning occurs, if $T \geq \chi^2_\alpha(M-1)$,
- Local wall-thinning does NOT occur, if $T < \chi^2_\alpha(M-1)$,

Where, $\chi^2_\alpha(M-1)$ means χ^2 -distribution whose degree of freedom is $M-1$, and the level of significance is α.

3.3. Continuous variables uniformity test (CVUT) method

BVUT uses the locational grouping and binomial variables for thinning values. In this method, the local thinning is estimated using locational grouping and continuous variables, not binomial variables. As shown in Fig. 10, if the thinning measurement data in each group appear to be similar to other groups, we can estimate that the local thinning does not occur.

Using the thinning measurement data itself, basically the estimation logic is the same as one-way ANOVA explained in Section 2.2. The EPRI's approach considered the measurement time as the treatment, but we can consider the locational group as the treatment to estimate local thinning. Therefore, the same test statistics, f shown in Eq. (1) and the same estimation criteria can be used in this approach, with exception as follows:

Table 2
Test cases for constructing estimation accuracy maps.

Parameter	Unit	Cases
Thinning area	% of total area	6 (5–30%, interval of 5%)
Max. thickness reduction	% of nominal thickness	6 (5–30%, interval of 5%)

$$MS_{tr} = \frac{\sum_{i=1}^{M} n_i(\overline{\Delta t}_{i\bullet} - \overline{\Delta t}_{\bullet\bullet})^2}{M-1},$$

$$MSE = \frac{\sum_{i=1}^{M}\sum_{j=1}^{n_i}(\Delta t_{ij} - \overline{\Delta t}_{i\bullet})^2}{\sum_{i=1}^{M}(n_i - M)}, F_\alpha\left(M-1, \sum_{i=1}^{M} n_i - M\right), \quad \text{(Eq. 8)}$$

where, Δt_{ij} is measured thinning values (thickness reduction values) of the j-th grid of the i-th group, n_i is the number of grids of i-th group and M is the number of groups.

3.4. Local wall-thinning estimation accuracies

In this section, the local wall-thinning estimation accuracies of the developed methods were examined by using the Monte-Carlo probability test. Virtual thinned piping components based on field experiences were constructed. Then, virtual thickness measurements data with random error were generated according to results of the previous study [4] for UT thickness measurement deviations. Applying the developed estimation methods to the virtual thinning data including various thinning depths and areas, the estimation accuracy maps for each method were constructed. Additionally, in order to compare the estimation accuracy with the EPRI's ANOVA method and TPM, the same probability test was conducted to the methods. Consequently, the estimation methods developed in this study identified to have better estimation accuracy than the methods used hitherto.

3.5. Virtual measurement data for Monte-Carlo probability test

In order to conduct Monte-Carlo probability test to examine the accuracy of the developed estimation methods, virtual measurement data were acquired for a piping component, whose nominal thickness and the outside diameter are 0.5 and 16 inches, respectively. The elbow is selected as the test piping component considering the field experiences for the nuclear power plant that the elbow was found to take up 65% of all inspected components.

In general, there are systematic thickness distributions for locations of elbows. In this virtual data, the thickness at intrados is 5% larger than the nominal thickness and that at extrados is 5% smaller than the nominal thickness. This kind of thickness distribution does not affect TPM, LDM, BVUT and CVUT because these methods use only thickness reduction data not thickness data itself. However, it

Table 1
Characteristics of virtual thinning measurement data for Monte-Carlo probability tests.

Item	Parameter	Values
Initial Pipe Thickness	Nominal(average) thickness, t_{nom}	0.5 inches
	Min. thickness(extrados)	$0.95t_{nom}$
	Max. thickness(intrados)	$1.05t_{nom}$
	Thickness distribution	$t_{ini}(\theta,z) = t_{nom}(1 - 0.05\cos(2\pi\theta))(\theta = 0$ at extrados)
Thinning Shape	–	See Fig. 11
Thickness Measurements	Measurement grids	156 points (circ. × axial = 12 × 13)
	Measurement error	Standard deviation = $0.0274t_{nom}$
		Normal distribution, $N(0,\sigma)$

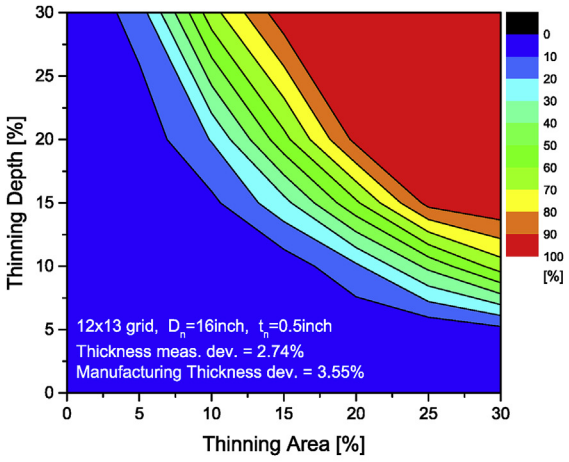

(a) EPRI's ANOVA method

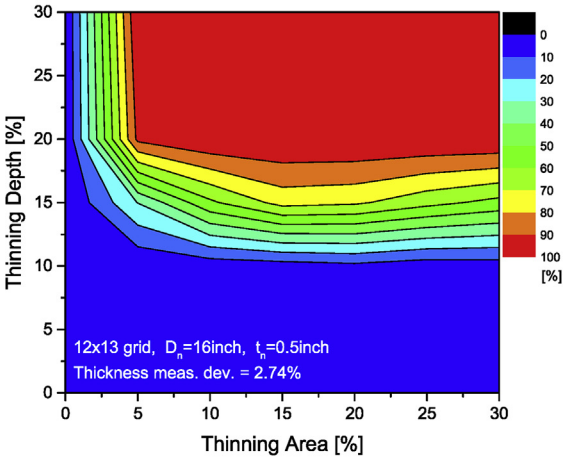

(b) Total point method (TPM)

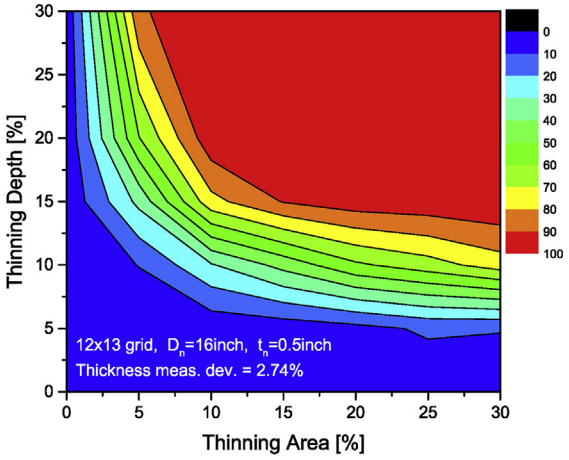

(c) Locational deviation method (LDM)

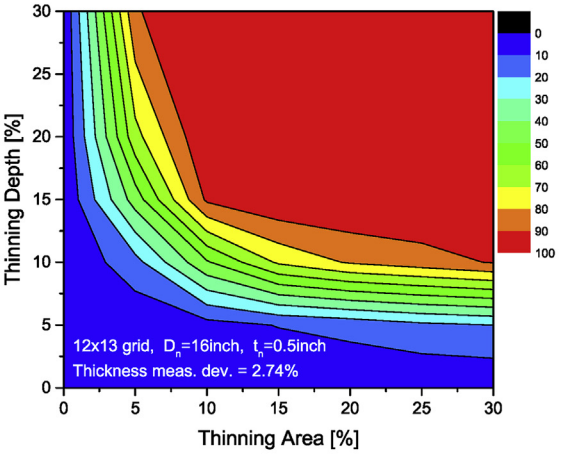

(d) Binomial variables uniformity test (BVUT)

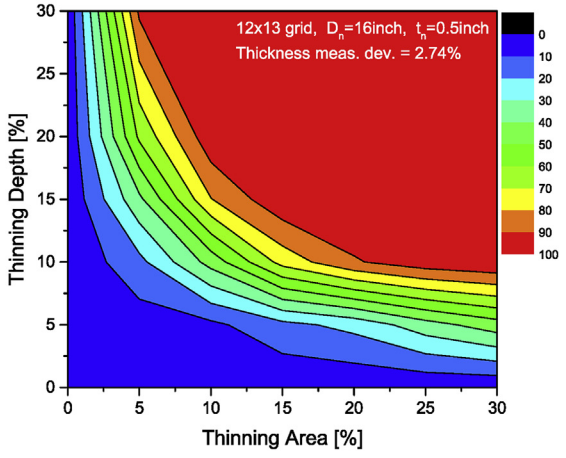

(e) Continuous variables uniformity test (CVUT)

Fig. 12. Probability test results for local thinning estimation accuracy.

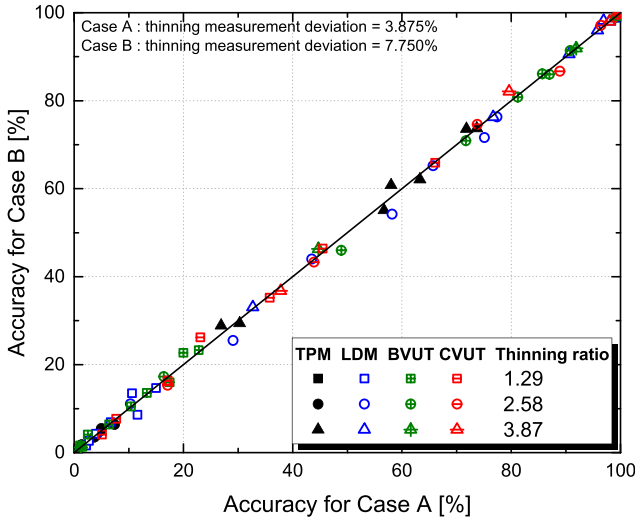

Fig. 13. Effects of thickness measurement errors (or thinning measurement deviations) on thinning estimation accuracies (thinning ratio = thinning depth/thinning measurement deviation).

is very important to the EPRI's ANOVA method because the deviation of the thickness in a component decreases f value of Eq. (1). The decreased f value makes estimation results to be 'NOT thinned' as explained in section 2.

Virtual thinning shapes considered in this Monte-Carlo probability test are elliptical and located at extrados of the elbow as shown in Fig. 11. Virtual thickness measurements are constructed at 156 grid points (circumferential × axial = 12 × 13) with measurement errors. The thickness measurement error is assumed to follow the normal distribution and the standard deviation is 2.74% of the nominal thickness. The measurement error is determined by considering the results of the previous study [4] for field experiences at the 16 inch diameter elbow.

In order to construct estimation accuracy maps, various thinning shapes are considered, which include 36 kinds of shape parameters (= 6 of thinning areas × 6 of thinning depths). For probability tests, 1000 components data were generated in each test case. The characteristics of virtual thinning measurement data for probability tests and the test cases for thinning shape are summarized in Tables 1 and 2, respectively.

3.6. Monte-Carlo probability test results

Fig. 12 shows the thinning estimation accuracies determined from Monte-Carlo probability tests. The estimation accuracies increased when the thickness reduction (thinning depth) increased, and the thinning area got wider in all estimation methods. The EPRI's ANOVA method shows the lowest accuracy in local thinning cases. The accuracy of TPM does not decrease with decreased thinning area, however, the accuracy rapidly decreases in the range of thinning depth lower than 20% of the nominal

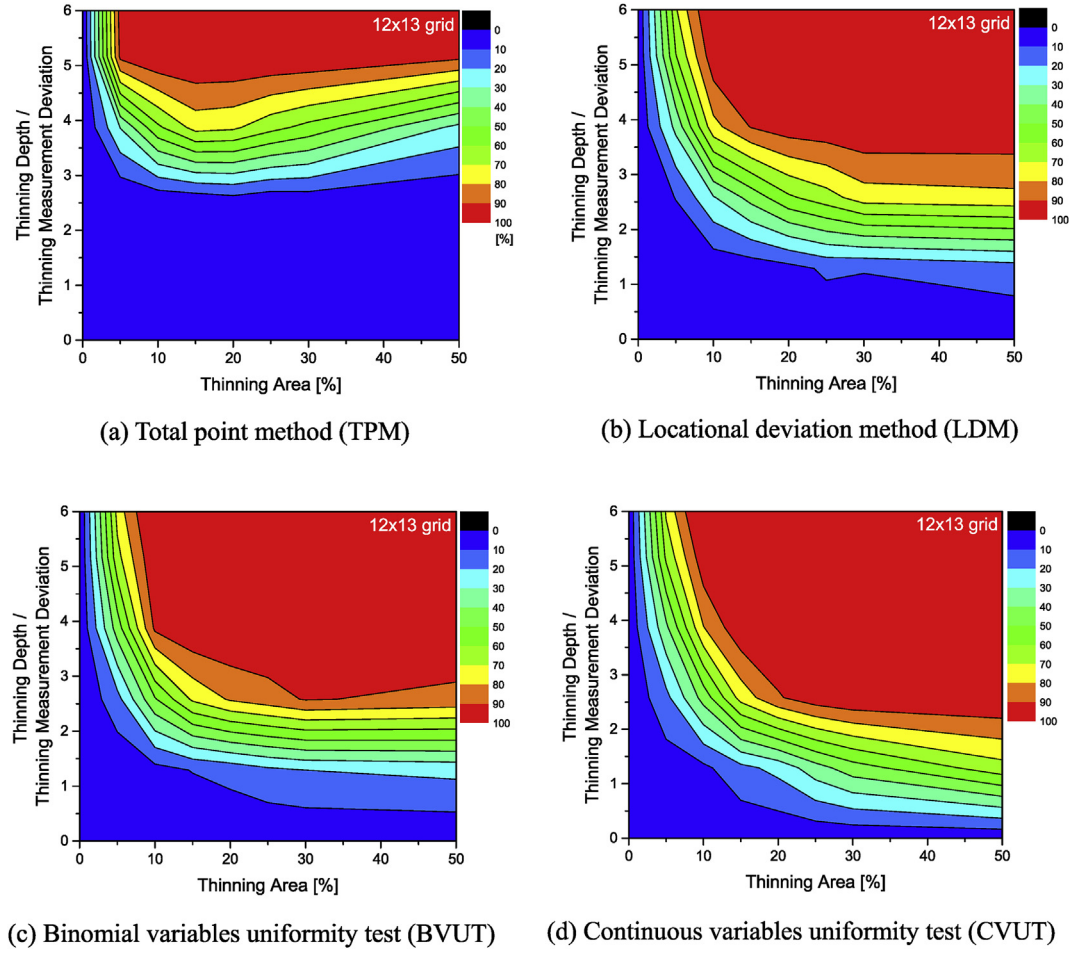

Fig. 14. Normalized accuracy maps for local thinning estimation.

thickness.

The newly developed estimation methods, LDM, BVUT and CVUT show better estimation accuracy than EPRI's methods. In the whole range of thinning depth and area, the accuracies of developed methods are higher than the EPRI's ANOVA method. In the range of 5–10% thinning area, the accuracies of developed methods are lower than TPM, however, are much higher than TPM in the range of larger thinning area. In BVUT and CVUT, the accuracy is dependent on the locational group setting. From simple examinations, 6 grid groups (circumferential × axial = 1 × 6) are used to maximize the estimation accuracy. Among the newly developed methods, the accuracy of CVUT is the highest in the whole range of thinning depth and area.

3.7. Normalized accuracy maps

Although Fig. 12 shows the accuracies of the thinning estimation methods, these graphs present the results only for a single value of thickness measurement deviation, 2.74%. If we understand the relation between the measurement deviation and the estimation accuracy, it is very helpful to recognize the confidence of the thinning estimation.

TPM, LDM, BVUT and CVUT use the thinning values determined from thickness measurement values. Therefore, the thinning estimation accuracy is a function of the deviation of thinning values not thickness values. If the thinning values are determined from two repeated thickness measurement values, the thinning measurement deviation can be calculated as follows:

$$\mathrm{Std}(Thin)^2 = 2 \cdot \mathrm{Std}(Thickness)^2, \quad \text{(Eq. 9)}$$

where, Std(*Thin*) is the standard deviation of the thinning measurement (thickness reduction measurement) values, and Std(*Thickness*) is the standard deviation of the thickness measurement values. Std(*Thickness*) can be determined from the thickness measurement values as follows, which was presented in the previous study [4].

$$\mathrm{Std}(Thickness)^2 = \frac{\sum_{i=1}^{n} \mathrm{Std}(Thickness)_i^2}{n}, \ \mathrm{Std}(Thickness)_i^2 = \frac{\sum_{j=1}^{k} (t_{ij} - t_{i,av})^2}{k-1}, \ \cdot t_{i,av} = \frac{\sum_{j=1}^{k} (t_{ij})}{k}, \quad \text{(Eq. 10)}$$

where, t_{ij} is the thickness measurement value at the i-th grid location in the j-th time. n and k are the number of grids and the time of measurements, respectively.

The considered estimation methods, TPM, LDM, BVUT and CVUT, are kinds of variance analysis, which are generally a linear estimator. In order to confirm the linearity of these methods, additional Monte-Carlo tests were conducted when the thickness measurement deviation is 5.48%, two times of the deviation of early Monte-Carlo tests. Consequently, two kinds of Monte-Carlo test results can be compared with each other, Case A (thickness measurement deviation = 2.74%, thinning measurement deviation = 3.875%) and Case B (thickness measurement deviation = 5.48%, thinning measurement deviation = 7.750%). Fig. 13 shows the accuracies determined from the Monte-Carlo tests of Case A and Case B. The thinning ratios (= thinning depth/thinning measurement deviation) are the same in Cases A and B, but the thinning measurement deviations are different. As shown in the figure, the estimation accuracies are the same at the same thinning ratio although the thinning measurement deviations are different.

Using this linearity of the estimation method, Fig. 12 can be converted into Fig. 14, wherein the 'Thinning Depth' is substituted to 'Thinning Depth/Thinning Measurement Deviation'. Using these accuracy maps shown in Fig. 14, we can estimate the confidence of the thinning estimation results when TPM, LDM, BVUT or CVUT are used. The confidence of estimations can be utilized when we have to make a decision for the next inspection or pipe repair times.

4. Conclusions

In order to prevent thinned pipe rupture event in NPP's secondary systems, it is very important to maintain a systematic pipe wall-thinning management program. Nevertheless, a systematic review of thinning estimation methods has not yet been made. In this paper, the characteristics of currently used thinning estimation methods were reviewed. Then, improved methods for local wall-thinning estimation were developed considering field experiences. Monte-Carlo probability tests were performed to quantify the estimation accuracy of the current and newly developed methods. The following conclusions are drawn from the results:

- When pipe wall thinning occurs in the whole area or most of the area, it can be easily identified by the EPRI's ANOVA and TPM currently in use.
- However, the estimation accuracy of the EPRI's ANOVA method is very low, especially for the case of local wall-thinning. TPM is more accurate than the EPRI's ANOVA method in the case of local thinning.
- The accuracy of the newly developed local thinning estimation methods is much better than the currently used estimation methods. Among three methods developed in this study, CVUT (continuous variable uniformity test) shows the best estimation accuracy.
- Using the linearity of the test estimator, the accuracy maps were presented. From this map, the estimation confidence can be quantified, which can help make a decision about the prediction of next inspection times or pipe repair times.

Declaration of competing interest

The authors declare that they have no known competing financial interests or personal relationships that could have appeared to influence the work reported in this paper.

References

[1] Electric Power Research Institute (Epri), Tr-1022295, Mentoring Guide for Flow-Accelerated Corrosion Engineers, 2010.
[2] Electric Power Research Institute (Epri), Tr-3002000563, Recommendations for an Effective Flow-Accelerated Corrosion Program (NSAC-202l-R4), 2013.
[3] Electric Power Research Institute (Epri), Electricite de France (Edf), and Siemens Ag Power Generation, Tr-106611-R1, Flow-Accelerated Corrosion in Power Plants, 2002.
[4] H. Yun, S.J. Moon, Y.J. Oh, Development of wall-thinning evaluation procedure for nuclear power plant piping – Part 1: Quantification of thickness measurement deviation, Nuclear Engineering and Technology 48 (No. 3) (2016) 820–830.
[5] Electric Power Research Institute (Epri), Chug Position paper No8, Determining Piping Wear Caused by Flow-Accelerated Corrosion from Single-Outage Inspection Data, 2006.
[6] Electric Power Research Institute (Epri), Chug Position Paper No 8, Determination of Measured Wear, 2010.
[7] Electric Power Research Institute (Epri), Tr-1020527, Evaluation of Multiple-Inspection Flow-Accelerated Corrosion Data on Unequal Grids, 2010.
[8] Electric Power Research Institute (Epri), Tr-1020528, Development of an Averaged Point-to-point Method for Inspection Data, 2010.
[9] Electric Power Research Institute (Epri), Tr-1018466, Optimization of FAC Inspections: BWR Feedwater Systems, 2008.
[10] Electric Power Research Institute (Epri), Tr-1018456, Least Squares Methods for Evaluating Inspection Data, 2008.
[11] Electric Power Research Institute (Epri), Tr-1019175, Statistical Methods for the Analysis of Multiple Inspection Flow-Accelerated Corrosion Data, 2009.

[12] Electric Power Research Institute (Epri), Chug Position Paper No 11, Investigation into Statistical Methods of Analyzing Multiple Inspection Data, 2010.
[13] Don Gusso, "Total Point Method Study", Presented at the 2010 CHUG Meeting, 2010.
[14] J. Horowitz, "Formal Statistical Methods", Presented at the 2010 CHUG Meeting, 2010.
[15] Young-Jin Oh, Hun Yun, Seung-Jae Moon, Kyunghee han and byeong-UK park, "Development of numerical algorithm of total point method for thinning evaluation of nuclear secondary pipes", Transactions of KPVP 11 (No.2) (2015).
[16] R.L. Scheaffer, J.T. McClave, Probability and Statistics for Engineers, third ed.", PWS-KENT Publishing Company, 1990.
[17] I. Miller, M. Miller, "John E. Freund's, Mathematical Statistics with Applications, seventh ed.", Pearson Education, Inc., Prentice Hall, 2004.